World Conference on Timber Engineering Oslo 2023

PERFORMANCE VERIFICATION AND TRIAL DESIGN FOR HIGH-RISE TIMBER FRAME BUILDINGS WITH BUCKLING-RESTRAINED BRACE PART 2: ANALYSIS OF THE TRIAL DESIGN BUILDING

Ryota Minami[1], Toshio Maegawa[2], Taisuke Nagashima[3], Kazuki Tachibana,[4] Hiroki Nakashima,[5] Nobuhiko Akiyama,[6] Yoshihiro Yamazaki,[7] and Takahiro Tsuchimoto[8]

ABSTRACT: Demand has recently emerged for large-scale structures made of timber. In earthquake-prone areas, such structures must feature adequate bearing capacity against major earthquakes. Part 1 of our research in this area entailed studies of methods to strengthen the bearing capacity of timber structures against the forces generated by major earthquakes. The work described in this paper confirms the seismic performance of a 10-story timber building designed by these methods. Analysis confirmed that the suggested methods strengthen the bearing capacity of large timber buildings against the forces generated by major earthquakes.

KEYWORDS: High-rise timber frame building, trial design, nonlinear dynamic analysis, buckling-restrained brace

1 INTRODUCTION

In earthquake-prone areas, structures made of timber tend to suffer significant damage when subjected to earthquake forces. For this reason, in Japan, virtually all medium- and large-scale structures are made of reinforced concrete or steel. However, various recent trends, including environmental issues, have generated demand for medium- and large-scale structures made of timber.

Medium- and large-scale buildings made of steel often incorporate buckling-restrained braces (BRBs) to boost bearing capacity against earthquake forces [1]. BRBs provide significant energy absorption capacity. BRBs incorporated into medium- and large-scale timber frame buildings should shoulder a significant share of the earthquake energy generated and improve building energy absorption capacity. This study assumes a 10-story timber frame building incorporating BRBs in Japan and proposes methods for achieving these design goals. The study also confirms the validity of these methods.

Building a 10-story timber frame building incorporating BRBs also requires sufficiently strong connections between beams or columns and the BRBs. This is due to the considerable strength and stiffness of the BRBs compared to timber constructions. It also requires column base connections with sufficient strength due to the large pull-out forces that can occur at the column base connections of buildings incorporating many braces or shear walls. In Part 1, we proposed multi knife plate steel dowel connections between beams or columns and BRBs (Figure 1) and glued-in rod (GIR) connections for the column base. To confirm the performance of these connections, we performed vertical loading tests of multi knife plate steel dowel connections, cyclic loading tests of timber frames with BRBs, and cyclic loading tests of column base connections with GIR.

This paper describes the trial of a seismic design for a 10-story timber frame building incorporating BRBs and using the connections proposed in Part 1. Our results confirmed their effectiveness, even for a 10-story timber frame building incorporating BRBs. The results reported here confirm the validity of incorporating BRBs in high-rise timber frame buildings.

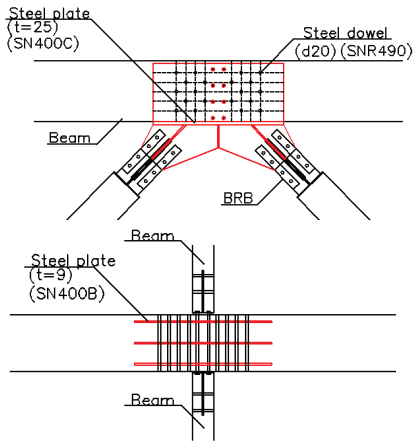

Figure 1: *Multi knife plate steel dowel connection proposed in Part 1*

[1] Ryota Minami, M. Eng., Kumagai Gumi, Japan, ryota.minami@ku.kumagaigumi.co.jp
[2] Toshio Maegawa, Chief Researcher, Kumagai Gumi, Japan, tmaegawa@ku.kumagaigumi.co.jp
[3] Taisuke Nagashima, PhD Eng., Chief Researcher, Sumitomo Forestry, Japan, tsk-naga@sfc.co.jp
[4] Kazuki Tachibana, M. Eng., Sumitomo Forestry, Japan, tachibana_kazuki@star.sfc.co.jp
[5] Hiroki Nakashima, M. Eng., Sumitomo Forestry, Japan, nakashima_hiroki@star.sfc.co.jp
[6] Nobuhiko Akiyama, Dr.Agr., Senior Researcher, Building Dept., NILIM, MLIT, Japan, akiyama-n92rg@mlit.go.jp
[7] Yoshihiro Yamazaki, Dr. Eng., Senior Research Engineer, Building Research Institute, Japan, y_ymzk@kenken.go.jp
[8] Takahiro Tsuchimoto, Dr. Agr., Chief Research Engineer, Building Research Institute, Japan, tutti@kenken.go.jp

https://doi.org/10.52202/069179-0387

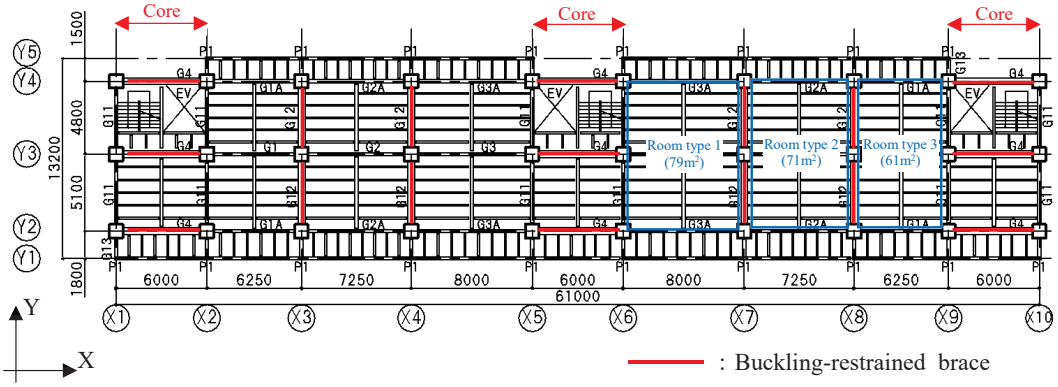

Figure 2: *Plan view of trial design building*

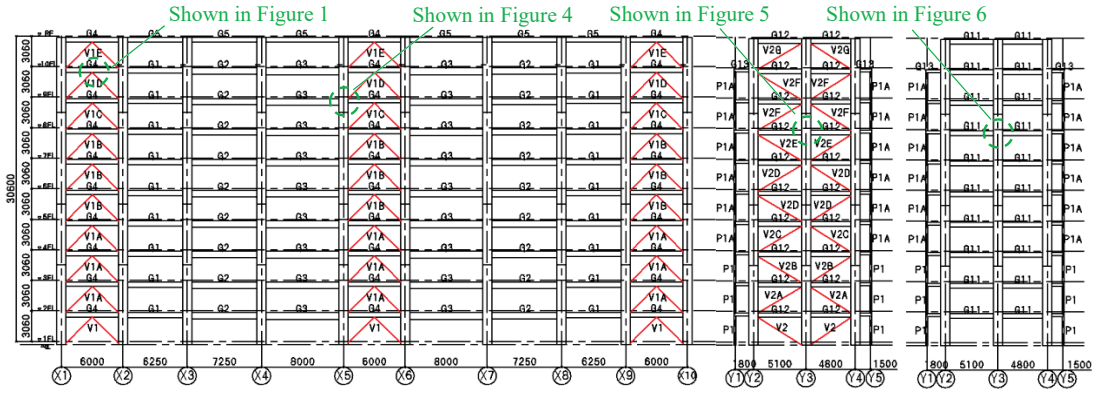

Figure 3: *Frame diagram of the trial design building (Left: Y2, Y3, Y4, Center: X3, X4, X7, X8, Right: other axles)*

2 TRIAL DESIGN BUILDING

2.1 TRIAL DESIGN BUILDING PLANS

Figures 2 and 3 show the plan view and frame diagram of the trial design building. In this paper, only the upper structure is considered. The building is assumed to be used for residential. BRBs are installed in the core (along the X direction) and between the rooms (along the Y direction). Columns and beams are made of glued laminated timber (GLT).

2.2 CONNECTIONS

Figures 4 and 5 show the beam-column connections at which the BRBs are attached. Figure 1 shows the connection between beams and BRBs. In these connections, beams, columns, and BRBs are connected via multi knife plate steel dowel connections. Figure 6 shows other beam-column connections; here, beams and column are connected with bolts and steel dowels due to the perpendicular orientation relative to the connections shown in Figures 4 and 5. In the connections shown in Figures 4 and 5, the steel plate holes of the beams into which the steel dowels are inserted are long. The steel dowels configured parallel to the direction of the grain are not subject to forces perpendicular to the direction of the grain; the steel dowels configured perpendicular to the direction of the grain are not subject to forces parallel to the direction of the grain.

2.3 COLUMN BASE CONNECTIONS

Figures 7 and 8 show the column base connections of the trial design building. Timber column and steel shoes are connected with the GIR connections proposed in Part 1. In this connection, reinforcement bars D29 are inserted and a plasticized section (φ22) is provided to ensure the uniform distribution of forces for the reinforcement bars. Steel shoes and foundations are connected with anchor bolts. In the trial design building, the column base connections in X1, X2, X5, X6, X9, and X10 are Type A (Figure 7). The others are Type B (Figure 8).

2.4 FLOOR SLABS AND CEILINGS

Figure 9 shows the floor slab and ceiling for an apartment in the trial design building. The dead loads are 2,270 N/m^2 (floors 2 to 6) and 1,880 N/m^2 (floors 7 to 10). Figure 10 shows the floor slab and ceiling for the rooftop. Figure 11 shows the floor slab and ceiling for the corridor. The dead load for the rooftop is 1,120 N/m^2; the dead loads for the corridor are 1,930 N/m^2 (floors 2 to 6) and 1,540 N/m^2 (floors 7 to 10).

The design value assumed for the floor slabs and beams live loads on these floor slabs is 1,800 N/m^2. The design value assumed for the frame members is 1,300 N/m^2; and the design seismic load assumed is 600 N/m^2 [2].

https://doi.org/10.52202/069179-0387

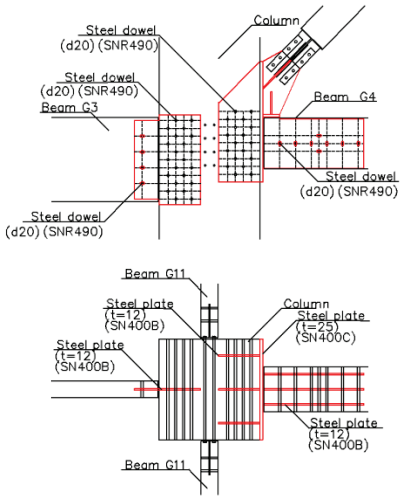

Figure 4: *Beam-column connection at which BRB is attached (X direction)*

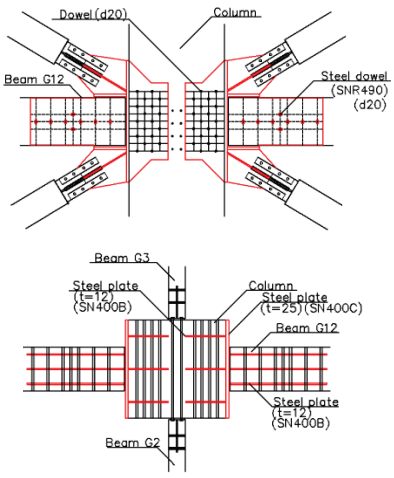

Figure 5: *Beam-column connection at which BRB is attached (Y direction)*

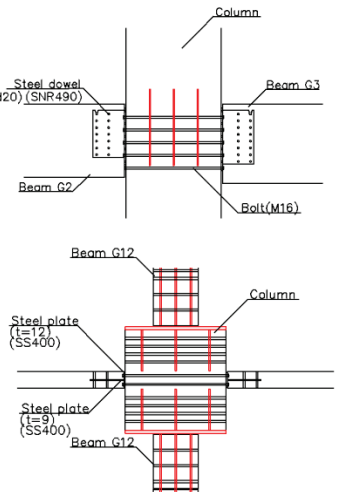

Figure 6: *Beam-column connection at which no BRB is attached*

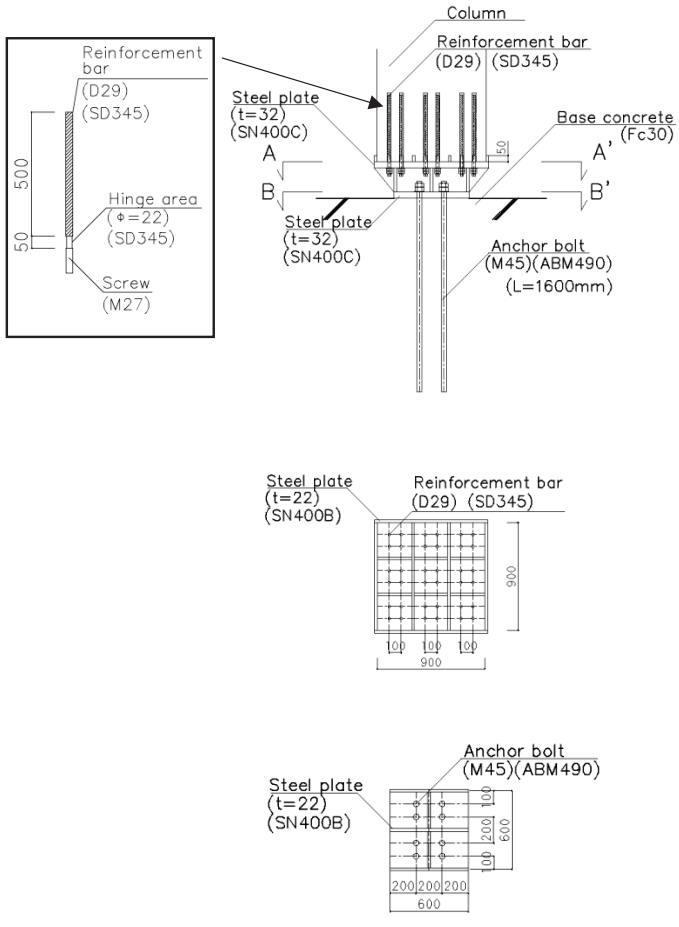

Figure7: *Column base connection (Type A)*

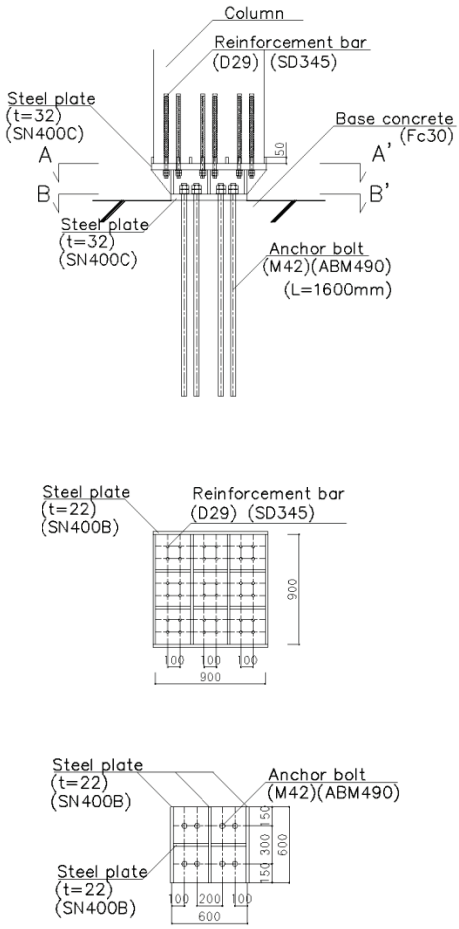

Figure 8: *Column base connection (Type B)*

https://doi.org/10.52202/069179-0387

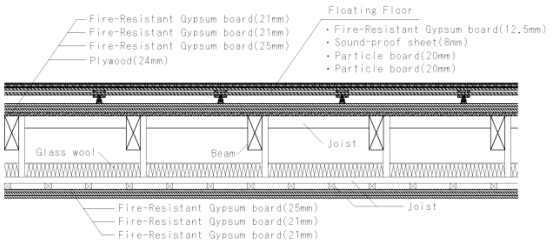

(a) Floors 2 to 6

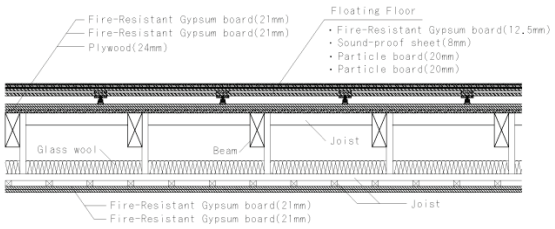

(b) Floors 7 to 10

Figure 9: *Floor slab and ceiling for apartments*

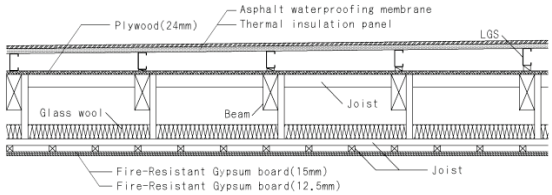

Figure 10: *Floor slab and ceiling for the rooftop*

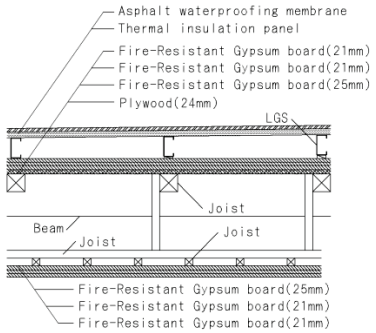

(a) Floors 2 to 6

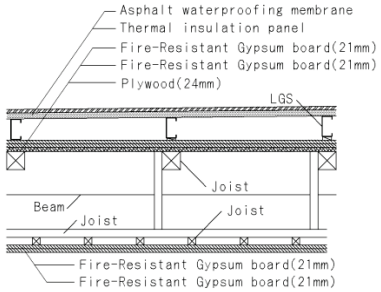

(b) Floors 7 to 10

Figure 11: *Floor slab and ceiling of the corridor*

3 ANALYSIS METHOD

3.1 SEISMIC DESIGN METHOD [3]

The building discussed in this paper is designed to satisfy the structural requirements specified by the Response and Limit Capacity Method, a Japanese code. This code requires verification of dead, live, snow, wind, and seismic loads. This paper considers only seismic loads. Seismic load verification requires drift pushover analysis, a method of nonlinear static analysis that involves increasing lateral loads in increments as shown in Figure 12 and checking the following criteria:

(a) Damage limit

This criterion is used to verify that damage caused by rare large-scale earthquake motions remains within the allowable range. In this paper, the damage limit is defined as the state in which the stress attributable to the lateral seismic load exceeds the temporary allowable stress (2/3 of material strength for timber members and yield strength for steel members) or at which the maximum interstory drift angle exceeds 1/200 rad. The lateral seismic shear force at the damage limit calculated by drift pushover analysis should exceed the lateral seismic shear force given by the following equation:

$$P_{di} = S_d B_{di} Z G_s m_i \quad (1)$$

(b) Safety limit

This criterion is used to verify that the building will not collapse when subjected to extremely rare large-scale earthquake motions. In this paper, the safety limit is defined as the state in which the maximum interstory drift angle exceeds 1/60 rad. The stress attributable to the lateral seismic loads at the safety limit should not exceed the material strength. The lateral seismic shear force at the building safety limit given by drift pushover analysis should exceed the lateral seismic shear force given by the following equation:

$$P_{si} = F\, S_s B_{si} Z G_s m_i \quad (2)$$

where S_d is the acceleration response at the damage limit on engineering bedrock; B_{di} is the acceleration distribution factor at the damage limit (first mode participation vector); Z is the seismic hazard zoning factor,; G_s is the surface soil amplification factor; m_i is weight of the i-th story; F is the acceleration reduction factor due to damping at the safety limit; S_s is the acceleration response at the safety limit on engineering bedrock; and B_{si} is the acceleration distribution factor at the safety limit (first mode participation vector).

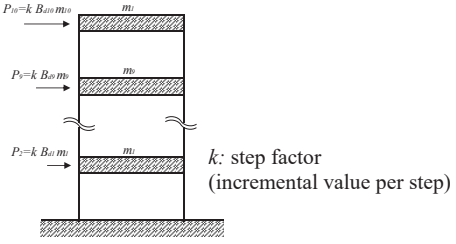

Figure 12: *Distribution of lateral force*

https://doi.org/10.52202/069179-0387

S_d and S_s are as in Figure 13.

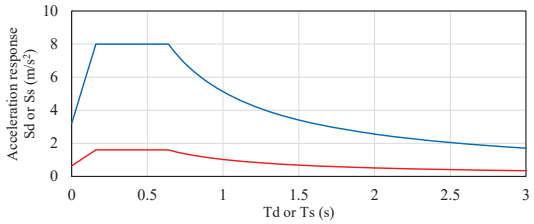

Figure 13: *Acceleration spectrum* $\boldsymbol{S_d}$ *and* $\boldsymbol{S_s}$

G_s is given by the following equation:

$$G_s = \begin{cases} 1.5 \quad for\ T < 0.64 \\ 1.5T/0.64 \quad for\ 0.64 \le T < 0.864 \\ 2.025 \quad for\ 0.864 \le T \end{cases} \qquad (3)$$

where $T = T_d$ when calculating P_{di} and $T = T_s$ when calculating P_{si}.

F is given by the following equation:

$$F = 1.5/(1 + 10\zeta) \qquad (4)$$

T_d and T_s are the response period at the damage limit and safety limit obtained by evaluating story stiffness and mass from the drift pushover analysis results and replacing the building with a 1DOF model, as shown in Figure 14. ζ is the damping ratio of the building given by the following equation:

$$\zeta = (\Delta s \cdot Q_d)/(\Delta d \cdot Q_s) \qquad (5)$$

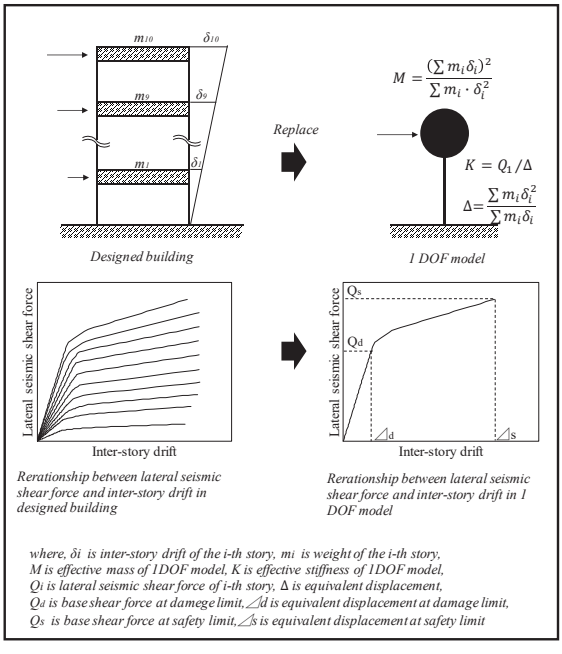

Figure 14: *Method to replace the building with 1DOF*

In addition to verification by the Response and Limit Capacity Method, the building performance upon the input of extremely rare large-scale earthquake motions is confirmed via time history analysis, accounting for P-Δ effects. Figure 15 shows the input earthquake ground motions. These are extremely rare large-scale earthquake motions as defined under Japanese Building Standard Law, which simulates earthquakes using random phase spectra (AW1-L2), the phase spectra specified in HACHINOHE 1968 NS (AW2-L2) and JMA KOBE NS (AW3-L2). The acceleration spectra for the engineering bedrock are shown in Figure 13 (S_s).

The analyses assume a rigid floor assumption and were performed using midas iGen V.920R1x.

3.2 NUMERICAL ANALYSIS MODEL

Figures 16 to 19 show numerical analysis models of the connections shown in Figure 1 and Figures 4 to 8.

In Figures 16 and 17, multi knife plate steel dowel connections are modelled by shear springs (parallel to the direction of the grain and perpendicular to the direction of the grain) and by rotational springs. The stiffness and yield strength values are calculated by the method proposed in Part 1. Knife plate steel dowel connections with long holes are not subject to bending moments and modelled with pin connections. For beam-column connections at which no BRB is attached, the knife plate steel dowel connection in the column is assumed to be rigid due to the negligible influence on building performance during an earthquake.

The connection in Figure 18 is modelled with pin connections since connections incorporating bolts and steel dowels have low stiffness.

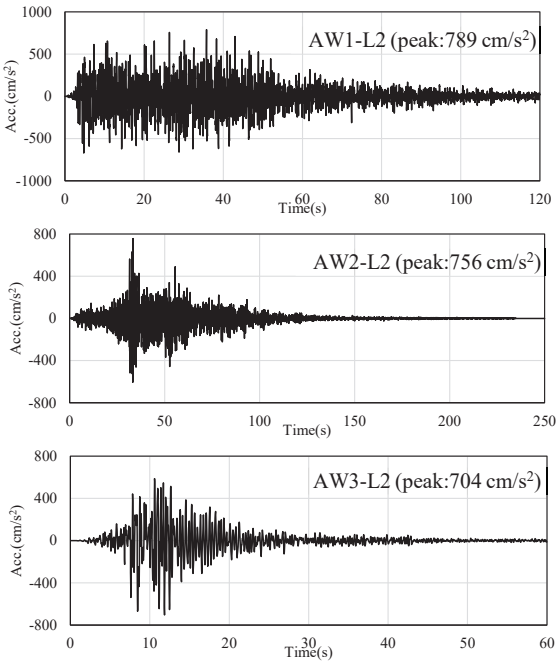

Figure 15: *Accelerations of input earthquakes*

https://doi.org/10.52202/069179-0387

In Figure 19, connections with GIR are modelled by a multi-spring model. (The values for stiffness and yield strength of the spring are given in Part 1.) Connections with anchor bolts are modelled with a multi-spring model. The values for spring stiffness are given by the following equations:

$$k_b = n_b A_b E_b / L \quad (6)$$

$$k_c = B_s \, s \, E_c / L \quad (7)$$

where k_b is the stiffness of the anchor bolt spring; k_c is the stiffness of the base concrete bearing spring; n_b is the number of anchor bolts; A_b is the cross section area of the anchor bolts; E_b is the elastic modulus of the anchor bolts; L is the length of the anchor bolts; B_s is the width of the steel shoe; s is the distance between the springs (= 50 mm); and E_c is the elastic modulus of the base concrete.

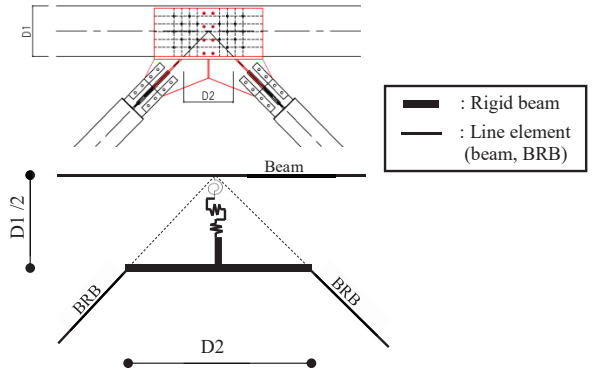

Figure 16: *Numerical analysis model for connection between beam and BRBs*

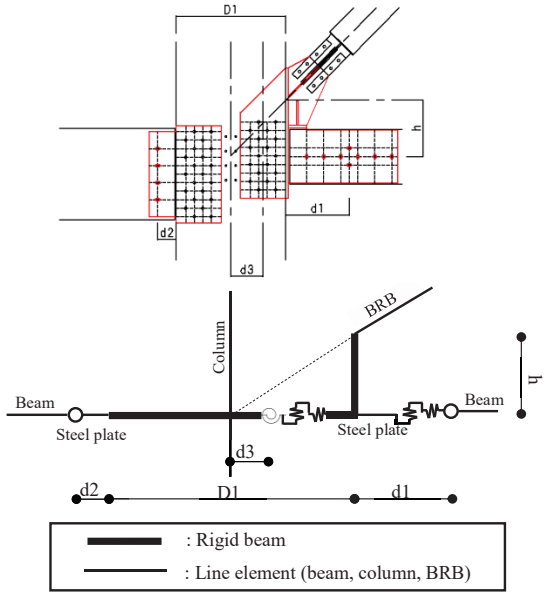

Figure 17: *Numerical analysis model for beam-column connection at which BRB is attached*

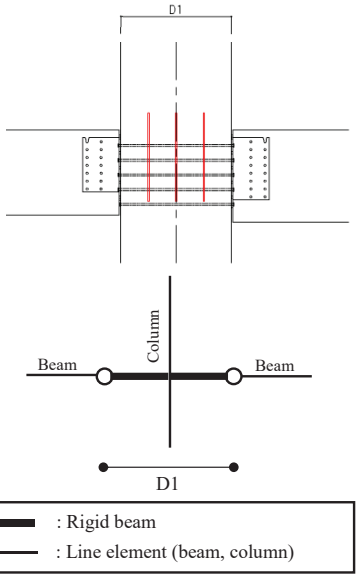

Figure 18: *Numerical analysis model of beam-column connection where BRB is not attached*

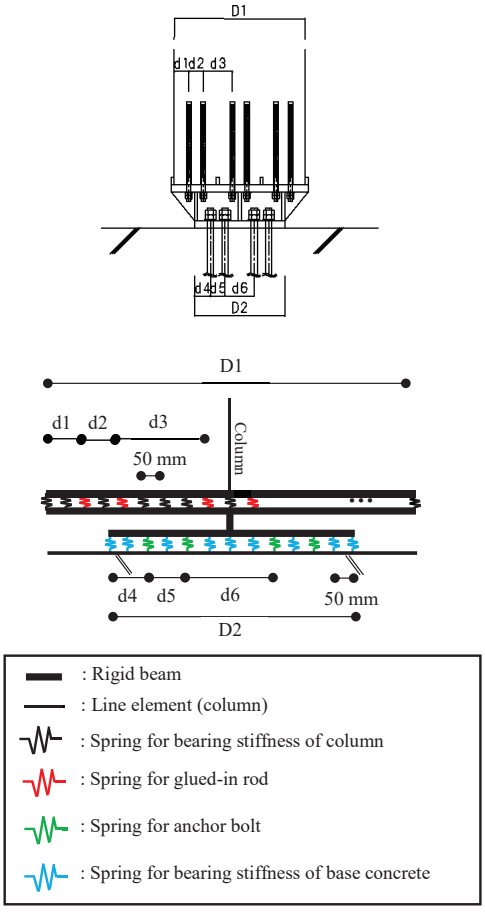

Figure 19: *Numerical analysis model for column base connection*

https://doi.org/10.52202/069179-0387

4 RESULTS OF ANALYSIS

4.1 STRUCTURAL MEMBERS

Tables 1 and 2 present the properties of the structural members of the trial design building as determined by analysis. Figures 2 and 3 show the component layout.

Table 1: *Column and beam properties*

Indicators	Story	Sections	Width × Length (mm)	Strength class in JAS
Column	All	C1	900 × 900	E105-F300 [4]
	1F - 3F	P1	210 × 210	
	4F - 9F	P1A	180 × 180	
Beam	2F - 7F	G1	150 × 600	
		G2	150 × 720	
		G3	150 × 780	
		G1A	150 × 510	
		G2A	150 × 630	
		G3A	150 × 690	
	8F - 10F	G1	150 × 540	
		G2	150 × 690	
		G3	150 × 750	
		G1A	150 × 480	
		G2A	150 × 600	
		G3A	150 × 650	
	RF	G5	150 × 480	
	ALL	G4	400 × 450	
		G11	105 × 480	
		G12	400 × 450	

Table 2: *BRB properties*

Sections	Width × Length (core plate in plastic zone) (mm)	Yield stress of steel materials for core plate (N/mm^2)	Yield load (kN)
V1	12 × 115	235	615
V1A	12 × 100		530
V1B	9 × 110		446
V1C	9 × 90		263
V1D	6 × 100	325	195
V1E	6 × 65		127
V2	9 × 120	355	738
V2A	12 × 128	325	952
V2B	16 × 135	235	955
V2C	19 × 140		1165
V2D	12 × 155		840
V2E	12 × 135		728
V2F	9 × 105	325	307
V2G	6 × 90		176

4.2 RESULTS OF PUSHOVER ANALYSIS

Figures 20 to 23 show the relationship between the interstory drift angle and lateral seismic shear force calculated by drift pushover analysis. In Figures 20 and 21, the damage limit state is the step at which the stress attributable to the lateral load exceeds the temporary allowable stress for the first time. In Figures 22 and 23, the safety limit state is the step at which the maximum interstory drift angle exceeds 1/60 rad for the first time.

From Figures 20 and 21, assuming the cross section shown in Tables 1 and 2, the lateral seismic shear capacity at the damage limit of the trial design building exceeds the lateral seismic shear force in Equation (1); the maximum interstory drift angle does not exceed 1/200 rad. In both the X- and Y- directions, the BRBs are the first structural members to exceed the temporary allowable stress value. From Figures 22 and 23, assuming the cross section shown in Tables 1 and 2, the lateral seismic shear capacity at the safety limit of the trial design building exceeds the lateral seismic shear force given by Equation (2). It was confirmed that the stress attributable to the lateral seismic load in the timber members does not exceed the material strength. Damping ratio ζ in Equation (5) is 15.1% in the analysis for the X-direction and 14.3% in the analysis for the Y-direction. Since the BRBs yielded, significantly high damping was observed. This is consistent with the design philosophy of this building, which is to improve the energy absorption capacity of the building by adopting BRBs.

Figure 24 shows the maximum value of the grain stress at the multi knife plate steel dowel connection between the beam and the BRBs (Figure 1) in this building at the safety limit calculated by pushover analysis for the X-direction. Figure 25 shows the maximum value of the grain stress at the multi knife plate steel dowel connection between the column and the BRBs (Figure 5) in this building at the safety limit calculated by pushover analysis for the Y-direction. They show the stress at multi knife plate steel dowel connections at which the BRBs are arranged in a K-shape does not exceed the temporary allowable stress at the safety limit. In the multi knife plate steel dowel connections used in this building, the greatest stress arises in connections at which the BRBs are arranged in a K-shape. This shows that the connections between the timber structures and the BRBs proposed in Part 1 remain reliable even in a 10-story timber frame building incorporating BRBs.

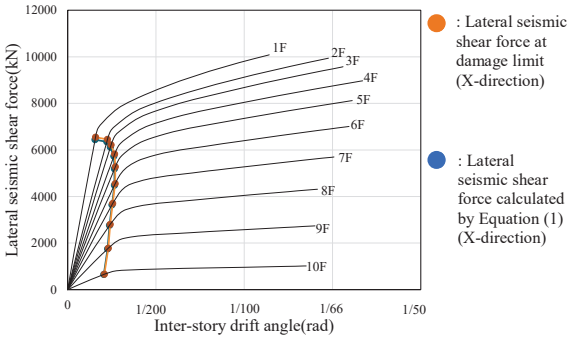

Figure 20: *Relationship between lateral seismic shear force and inter-story drift angle at damage limit in X direction analysis*

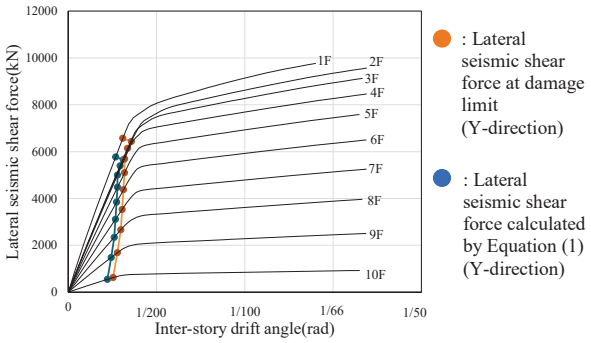

Figure 21: *Relationship between lateral seismic shear force and interstory drift angle at damage limit in Y direction analysis*

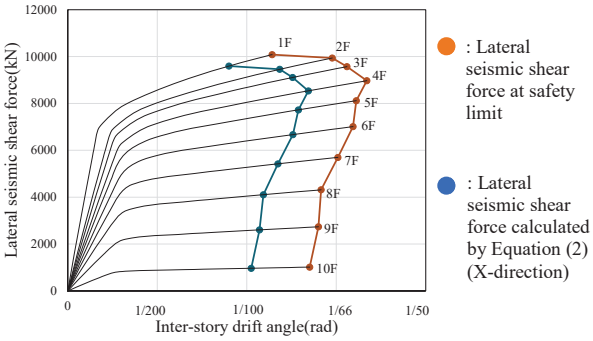

Figure 22: *Relationship between lateral seismic shear force and interstory drift angle at safety limit in X direction analysis*

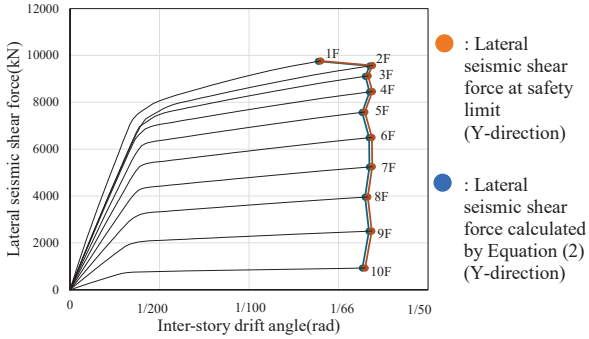

Figure 23: *Relationship between lateral seismic shear force and interstory drift angle at safety limit in Y direction analysis*

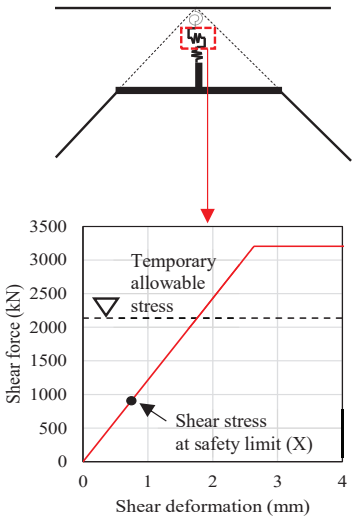

Figure 24: *Maximum grain direction stress at the multi knife plate steel dowel connection between beam and BRBs*

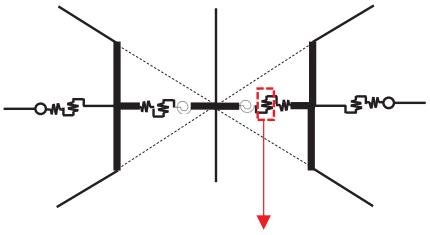

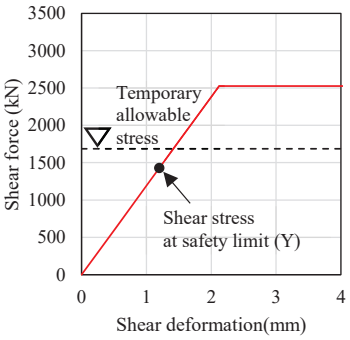

Figure 25: *Maximum grain direction stress at the multi knife plate steel dowel connection between column and BRBs*

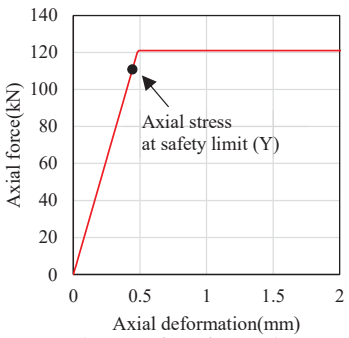

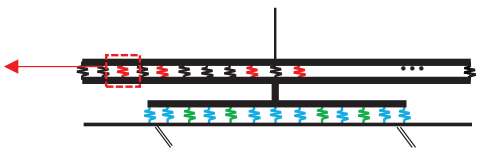

Figure 26: *Maximum axial stress of reinforcing bar in GIR connections*

https://doi.org/10.52202/069179-0387

Figure 26 shows the maximum axial stress for the reinforcing bar in GIR connections (Figures 7 and 8) attributable to the lateral seismic force at the safety limit (in both the X and Y directions). Figure 25 shows that the stress on the reinforcement bar does not exceed the yield strength for the plasticized section at the safety limit. Figure 27 shows M-N interaction curves for GIR and anchor bolt connections (Figures 7 and 8). It indicates that the anchor bolt connections yield before the GIR connection at the column base connection of this building. This means that the GIR connection proposed in Part 1 remains reliable even for a 10-story timber frame building incorporating BRBs in which anchor bolt connections are designed to yield before GIR connections.

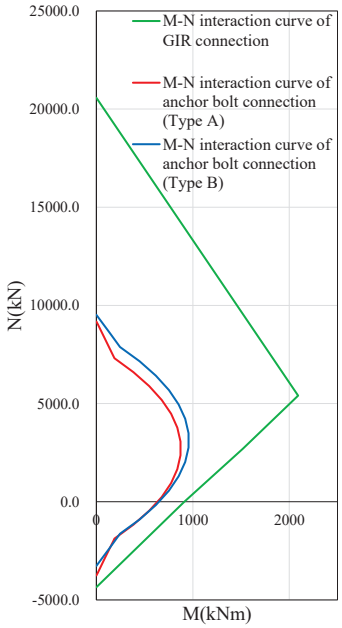

Figure 27: *M-N-interaction curves of GIR connection and anchor bolt connection*

4.3 RESULTS OF TIME HISTORY ANALYSIS

Figure 28 shows the maximum interstory drift angle of the trial design building obtained via time history analysis. Figure 28 shows that the maximum interstory drift angle of the trial design building given by time history analysis does not exceed 1/60 rad, which is assumed to be the interstory drift angle at the safety limit in the drift pushover analysis. It was also confirmed that the stress attributable to the lateral seismic load in the timber member does not exceed the material strength via time history analysis.

Figures 29 and 30 show the maximum value of the grain stress at the multi knife plate steel dowel connection between the beam and the BRBs (Figure 1) and the maximum value of the grain stress at the multi knife plate steel dowel connection between the column and the BRBs (Figure 5). Figure 31 shows the maximum axial stress on the reinforcing bar in the GIR connections, as in the previous section. Figures 29 to 31 show the results of the time history analysis, confirming the effectiveness of the connections proposed in Part 1.

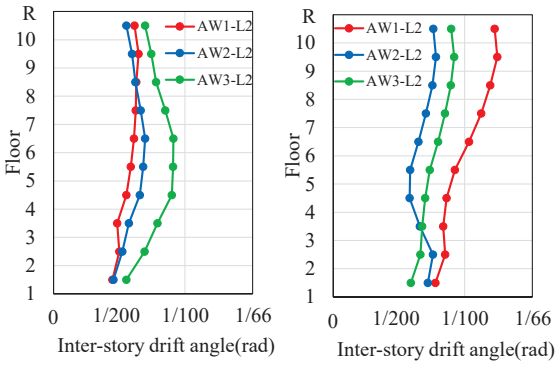

(a) X-direction *(b) Y-direction*

Figure 28: *Maximum inter-story drift angle*

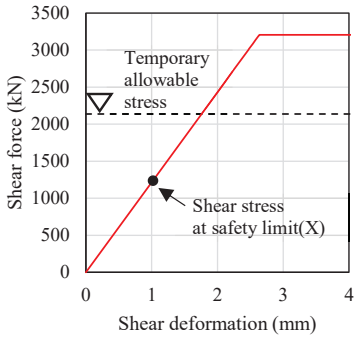

Figure 29: *Maximum grain direction stress at the multi knife plate steel dowel connection between beam and BRBs*

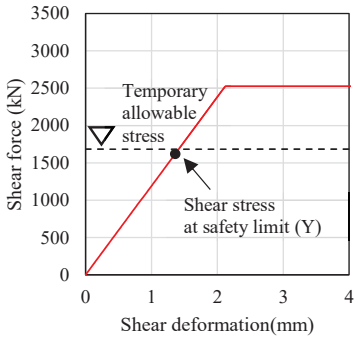

Figure 30: *The maximum grain direction stress at the multi knife plate steel dowel connection between column and BRBs*

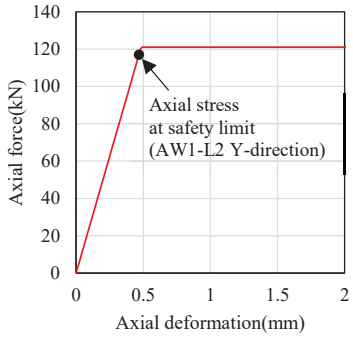

Figure 31: *Maximum axial stress on reinforcing bar in GIR connections*

5 CONCLUSIONS

This paper discusses aspects of trial seismic design for a 10-story timber frame building incorporating BRBs and using the connections proposed in Part 1.

Static analysis based on the Response and Limit Capacity Method and time history analysis confirmed that these BRBs will absorb considerable energy in the event of an earthquake and improve the bearing capacity of high-rise timber frame buildings. Our efforts also confirmed that the stress arising in multi knife plate steel dowel connections between BRBs and beams or columns and in GIR connections of column base connections proposed in Part 1 remains within the experimentally confirmed bearing capacity, thereby confirming the validity of the connections proposed in Part 1.

ACKNOWLEDGEMENTS

This research was conducted as part of “Innovative technology for maintenance and management of construction and infrastructure and for disaster prevention and mitigation” in Public/Private R&D Investment Strategic Expansion Program (PRISM) add-on item “ R&D Project for tall wood building for saving construction site of recovery housing“.

REFERENCES

[1] T. Takeuchi, A. Wada: BUCKLING-RESTRAINED BRACES AND APPLICATIONS, 2017.
[2] Architectural Institute of Japan: Recommendations for loads on buildings (2015), 2015.
[3] National Institute for Land and Infrastructure Management and others: Commentary on Structural Regulations of the Building Standard Law of Japan (2020), 2020.
[4] Architectural Institute of Japan: Standard for Structural Design of Timber Structures (2013), 2013.

https://doi.org/10.52202/069179-0387